Nanoscale Horizons

REVIEW

View Article Online
View Journal | View Issue

Cite this: *Nanoscale Horiz.*, 2017, 2, 135

Synthesis, optical properties and applications of light-emitting copper nanoclusters

Zhenguang Wang,[a] Bingkun Chen[ab] and Andrey L. Rogach*[a]

Received 24th January 2017,
Accepted 7th March 2017

DOI: 10.1039/c7nh00013h

rsc.li/nanoscale-horizons

Metal nanoclusters (NCs) containing a few to a few hundreds of atoms bridge the gap between nanoparticles and molecular compounds. The last decade evidenced impressive developments of noble metal NCs such as Au and Ag. Copper is an earth abundant, inexpensive metal from the same group of the periodic table, which is increasingly coming into focus for NC research. This review specifically addresses wet chemical synthesis methods, optical properties and some emerging applications of Cu NCs. As surface protecting templates/ligands play an important role in the stability and properties of Cu NCs, we classified the synthetic methods by the nature of the capping agents. The optical properties of Cu NCs are discussed from the point of view of the effects of the metal core, surface ligands and environment (solvents and aggregation) on the emission of the clusters. Applications of luminescent Cu NCs in biological imaging and light emitting devices are considered.

1. Introduction

Metal nanoclusters (NCs) containing a few to a few hundreds of atoms[1–3] bridge the gap between nanoparticles and molecular compounds, and often show molecule-like electrical and optical properties.[4–8] Intensive studies are focused on the synthesis and applications of noble metal NCs, mostly on Au and Ag. Cu belongs to the same group in the periodic table, and is an earth abundant, rather inexpensive metal widely used in industry. This review offers a summary on the wet chemical synthesis methods, optical properties and applications of Cu NCs, mostly considering rather recent publications in this area, which have appeared within the last decade. We do not include any gas phase fabrication methods of Cu NCs, and we have divided the chemical synthesis approaches into template-assisted and ligand-assisted wet chemical methods, as well as electrochemical synthesis and etching techniques.

[a] *Department of Physics and Materials Science and Centre for Functional Photonics (CFP), City University of Hong Kong, 83 Tat Chee Avenue, Kowloon, Hong Kong SAR, China. E-mail: andrey.rogach@cityu.edu.hk*
[b] *Beijing Key Laboratory of Nanophotonics and Ultrafine Optoelectronic Systems, School of Materials Science & Engineering, Beijing Institute of Technology, Beijing, 100081, China*

Zhenguang Wang

Zhenguang Wang is a PhD candidate at the Department of Physics and Materials Science, City University of Hong Kong. He received his Master's degree in Analytical Chemistry from Shandong University in 2013. His research focuses on the chemical synthesis and characterization of luminescent metal nanoclusters and semiconductor quantum dots, and their application in light emitting diodes and chemical sensors.

Bingkun Chen

Dr Bingkun Chen is a postdoctoral fellow in the laboratory of Beijing Engineering Research Center of Mixed Reality and Advanced Display at the Beijing Institute of Technology (BIT). He received his PhD degree in Materials Science from BIT in 2013, and worked as a postdoctoral researcher (Hong Kong Scholar Program) at the Department of Physics and Materials Science, City University of Hong Kong from 2014 to 2016. His research interests are focused on low-toxic semiconductor nanocrystals such as I–III–VI quantum dots, and aluminum hydroxide based materials for applications in light emitting diodes, solar cells and photo-catalysis.

The light-emission properties of Cu NCs are considered to be attractive,[9–11] while the reported photoluminescence (PL) quantum yields (QYs) still require further improvements. This review thus considers possible PL mechanisms of Cu NCs, and discusses the effects of the metal core, ligands and environment (solvents and aggregation) on their emission properties. Possible applications for luminescent Cu NCs are in the areas of chemical sensors, biological imaging and light emitting devices (LEDs), taking advantage of their bio-compatibility and low cost production. As two recent reviews have already considered analytical and chemical sensing applications of Cu NCs,[10,12] we will briefly mention the related information in the synthesis part of this review, while providing more in-depth treatment on biological imaging and LED applications in the respective subsections. The review ends with concluding remarks and an outlook for the flourishing field of Cu NC related research.

2. Synthesis of Cu NCs

The majority of Cu NCs are synthesized using wet chemistry methods, where Cu(II) ions are reduced to Cu atoms in solution, followed by clustering of Cu atoms.[9,10] To obtain stable Cu NCs, they should be protected from aggregation and oxidation, which is commonly achieved by selecting suitable surface ligands. In addition, suitable ligands are a key component for producing strongly luminescent Cu NCs, as the nature of the ligands can significantly affect their PL properties.[12–15] According to the methods used to fabricate and to maintain the small size of Cu NCs during the synthesis, we have classified the related literature reports into several categories, including template-assisted methods, ligand-assisted methods, electrochemical synthesis, and etching methods.

Andrey L. Rogach

Prof. Andrey L. Rogach is a Chair Professor of Photonics Materials and the founding director of the Centre for Functional Photonics at the City University of Hong Kong. He received his Diploma in Chemistry (1991) and PhD in Physical Chemistry (1995) from the Belarusian State University in Minsk, and worked as a staff scientist at the Institute of Physical Chemistry at the University of Hamburg, Germany, from 1995 to 2002. During 2002–2009, he held a tenured position of lead staff scientist at the Department of Physics of the Ludwig-Maximilians-Universität in Munich, where he completed his habilitation in Experimental Physics. His research focuses on the synthesis, assembly and optical spectroscopy of colloidal semiconductor and metal nanocrystals and their hybrid structures, and their use for photocatalytic and optoelectronic applications.

2.1. Template-assisted methods

In the template-assisted methods, a suitable template with a predetermined structure is utilized to bind Cu(II) ions first, which then become reduced into Cu atoms and clusters on the template, forming Cu NCs. Steric protection by the template helps to avoid aggregation of the NCs or their decomposition in solution. A number of templates including polymers, DNA, proteins and peptides have been employed for the synthesis of Cu NCs, which will be reviewed in the following sections.

2.1.1 Polymer templates. Appropriate functional groups on the polymer backbone can provide multiple binding sites for Cu(II) ions. In 1998, Crooks's group synthesized Cu NCs in the interior of poly(amidoamine) (PAMAM) starburst dendrimers.[16] The PAMAM dendrimer with hydroxyl surface groups was mixed with $CuSO_4$ in aqueous solution, followed by reduction of Cu(II) ions to Cu NCs by $NaBH_4$. Clusters with different numbers of constituting Cu atoms (from 4 to 64) could be obtained by varying the size of the host dendrimer (Fig. 1A).[17] Around the same time, Balogh and co-workers reported the synthesis of Cu NCs through the complexation of Cu(II) within PAMAM, followed by their reduction into zero-valent Cu clusters in methanol.[18] In 2001, McCarley's group prepared Cu(II)–poly(propylene imine) dendrimer complexes with a diaminobutane (DAB) core (DAB-Am_n-$Cu(II)_x$, $x = n/2$), which formed Cu NCs after reduction by $NaBH_4$ in methanol.[19] Zhang and co-workers reported the synthesis of Cu NCs by photoreduction under UV light irradiation of the Cu(II) aqueous solution, making use of the poly(methacrylic acid) template modified with pentaerythritol tetrakis 3-mercaptopropionate. Cu NCs with PL emission peaking at 630 nm (excited at 360 nm) were obtained.[20] Compared with other reduction methods, photoreduction is a low-toxicity, clean and less time-consuming approach,[21] which has also been employed for the synthesis of Au and Ag clusters.[20] Poly(ethylene glycol) functionalized by lipoic acid (LA-PEG_{750}-OCH_3) was also employed as a template to synthesize Cu NCs by reduction with $NaBH_4$,[22] showing blue PL emission peaking at 416 nm, with a PL QY of 3.6%. Pellegrino's group purposefully designed poly(ethylene glycol)-*block*-poly(propylene sulfide) for synthesizing Cu NCs by mixing this polymer with CuBr under inert gas protection in tetrahydrofuran (Fig. 1B).[14] The thiolate group of the PPS segment was used to capture and reduce Cu(II) ions into Cu(0), while the PEG

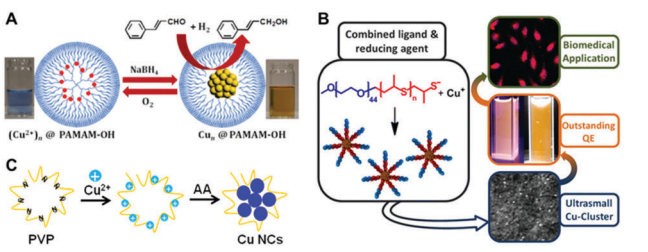

Fig. 1 Schematic illustration for the synthesis of Cu NCs using PAMAM (A), functionalized PEG (B) and PVP (C) as the template. (A) Reproduced with permission from ref. 17, Copyright 2013, American Chemical Society. (B) Reproduced with permission from ref. 14, Copyright 2015, American Chemical Society.

segment prevented aggregation of the resulting Cu NCs. After purification, Cu NCs showing PL emission peaking at 583 nm were obtained, with an outstanding PL QY of up to 67%, which is the highest number for Cu NCs reported so far.[14]

Polyethyleneimine (PEI), containing a large number of amine groups (primary, secondary, and tertiary), has been widely utilized as a template to synthesize metal nanoparticles. After mixing PEI with Cu(II) in an appropriate ratio, hydrazine hydrate[23] or ascorbic acid (AA)[24] has been used to reduce Cu ions into Cu(0) which forms clusters on the PEI chain, forming Cu NCs. The PEI-templated Cu NCs were easily water soluble and possessed reasonable stability under ambient conditions; they showed blue PL emission with PL QY ranging from 2.1% to 3.8%.[23–25] Importantly, their PL proved to be rather sensitive to external stimuli; based on this property chemical sensors for hydrogen peroxide,[23] ferric ions,[24] iodide,[26] pH[27] and Sudan dyes[27] have been developed. Poly(vinylpyrrolidone) (PVP), widely used as a surfactant to synthesize metal nanoparticles, contains amide groups, which easily bind with Cu(II) ions by interaction of lone electron pairs of N atoms with empty orbitals of Cu(II). Ghosh *et al.* synthesized Cu NCs in the presence of PVP using a two-step reduction approach.[28] Firstly, PVP and Cu(II) were mixed together in a saturated solution of NaCl, followed by the addition of AA to reduce Cu(II) to Cu(I). Then, dihydrolipoic acid (DHLA) was used to further reduce Cu(I) ions to Cu(0), resulting in the formation of Cu NCs. Tang and co-workers synthesized Cu NCs using a hydrothermal method using PVP as a template and formaldehyde as a reducing agent.[29] The resulting Cu NCs showed an excitation dependent PL emission peak ranging from 398 nm to 457 nm for the excitation wavelength changing from 310 to 390 nm, with a maximum PL QY of 13%. Our group introduced a one-pot method to synthesize Cu NCs, by reduction of Cu(II) ions supported on PVP using AA (Fig. 1C).[30] After incubation of the mixture of Cu(II), PVP and AA under room temperature, an intense blue PL emission (peaked at 423 nm) with a PL QY of 8% was observed, indicating the formation of Cu NCs.

2.1.2 DNA templates. Owing to their useful properties, such as molecule recognition, programmable sequence and robust geometric structure, DNA templates have been widely employed for the synthesis of metal NCs. Mokhir's group demonstrated that random double-stranded DNA (dsDNA) can be used to stabilize Cu NCs obtained by the reduction of Cu(II) ions with AA (Fig. 2A), which showed PL in the range of 580–600 nm (excited at 340 nm).[31] The PL intensity and the size of the resulting Cu NCs could be controlled by the length of dsDNA templates. Random single-stranded DNA (ssDNA) failed to support the formation of Cu NCs in their approach. Ouyang's group systematically studied the formation of Cu NCs on dsDNA templates by varying the sequence combinations,[32] and found that random sequences as well as several specific sequences failed to generate luminescent species, while adenine/thymine (AT) rich sequences generated Cu NCs with red PL. Employing diverse dsDNA with site-specific sequences, and combined together with the recognition ability of DNA to other molecules, chemical sensors for single nucleotide polymorphisms (SNPs),[33]

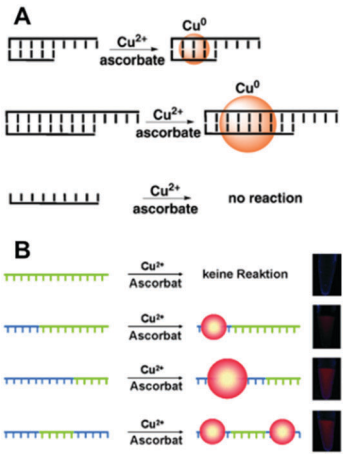

Fig. 2 Schematic illustrations of the synthesis of Cu NCs using dsDNA (A) and ssDNA (B) as templates. The green sequences stand for T bases of DNA. (A) Reproduced with permission from ref. 31, Copyright 2010, Wiley-VCH Verlag GmbH & Co. KGaA. (B) Reproduced with permission from ref. 13, Copyright 2013, Wiley-VCH Verlag GmbH & Co. KGaA.

genotypes of Duchenne muscular dystrophy,[34] DNA,[35] adenosine triphosphate (ATP),[36] nuclease enzyme,[37] lead ions (Pb^{2+}),[38] sulfide anions (S^{2-}),[39] thiols (glutathione (GSH), cysteine and homocysteine),[40] L-histidine,[41,42] alkaline phosphatase,[43] polynucleotide kinase activity,[44] microRNA,[45,46] and polymerization-mediated biochemical analysis[47] were developed. Wang's group employed different ssDNA templates to synthesize Cu NCs, including random ssDNA, poly(adenine) (poly A), poly(thymine) (poly T), poly(cytosine) (poly C), and poly(guanine) (poly G), as shown in Fig. 2B.[13] They found that only the use of a poly T based template resulted in the formation of luminescent Cu NCs, with a PL peak at around 600 nm at the excitation wavelength of 340 nm. Both the size and PL QY of the Cu NCs could be tuned by altering the length of the poly T sequence, with longer segments inducing the formation of larger clusters with higher PL QY. Other ssDNA molecules, including random ssDNA, poly A, poly C, and poly G based ones, failed to serve as templates for luminescent Cu NCs under the same reaction conditions. Similar observations have been reported by Wu's group,[48] which used ssDNA (poly A, poly T, poly C and poly G) as templates to synthesize Cu NCs and found out that only Cu NCs synthesized using poly T had PL emission peaked at 630 nm. They ascribed the selective formation of luminescent Cu NCs and the difference in NC size for different DNA sequences to the variation of binding affinity of Cu(I) intermediates formed during the reduction of Cu(II) to Cu(0) to the DNA bases. Among the four kinds of DNA bases, T showed the weakest binding ability to Cu(I), facilitating the reduction of Cu(I) to Cu(0), while G possessed the highest binding affinity towards Cu(I), preventing its reduction to Cu(0). Utilizing luminescent Cu NCs stabilized by ssDNA, chemical sensors for nucleases,[49] logic devices,[50] microRNA,[51] ATP,[52] and melamine[53] were developed.

2.1.3 Protein and peptide templates. Proteins, consisting of one or several amino acid residues, offer several functional chemical groups, such as amine- and carboxyl-groups, with a

strong ability to coordinate Cu(II) ions and fixing subsequently formed Cu(0) atoms on the protein backbone. Some proteins also possess reducing ability, due to the presence of thiol groups, and thus can work as both stabilizing and reducing agents for Cu NCs. Goswami and co-workers reported the synthesis of Cu NCs by using bovine serum albumin (BSA) as both the template and the reducing agent, as shown in Fig. 3A.[54] BSA was mixed with $CuSO_4$ in aqueous solution, followed by the addition of NaOH to promote the reduction of Cu(II) ions and their clustering into Cu NCs with blue emission (with excitation and emission peaks at 325 and 410 nm, respectively). Liao and co-workers reported a synthesis based on the addition of H_2O_2 solution into the BAS–$CuSO_4$ mixture.[55] In this work, H_2O_2 acted as an additive to increase the exposure of free amino groups in BSA, which can accelerate the formation of Cu NCs. Wang and co-workers synthesized BSA protected Cu NCs with the assistance of hydrazine hydrate used as a reducing agent.[56] The Cu clusters showed red emission (excitation at 524 nm and emission at 625 nm) with a PL QY of 4.1%, which was in strong contrast to the Cu NCs synthesized without adding hydrazine hydrate (blue emitting ones). The PL of the Cu NCs templated on BSA could be quenched by Pb^{2+},[54] Hg^{2+},[55] Cu^{2+},[57] 2,4,6-trinitrophenol (TNP),[58] and H_2O_2,[59] which was employed to develop corresponding chemical sensors. Other proteins were also used to synthesize Cu NCs, such as papain in combination with the reducing agent hydrazine hydrate,[60] which resulted in red emitting Cu NCs (excitation at 370 nm and emission at 620 nm) with a PL QY of 14.3%. Based on the same concept, Ghosh and co-workers synthesized Cu NCs templated by lysozyme, showing blue PL with a PL QY of 18%.[61] Yeast extract, which contains many natural components including proteins, carbohydrates and amino acids, was also employed as a template and at the same time as a reducing agent to synthesize Cu NCs.[62] A mixture of yeast extract and Cu(II) ions was refluxed for 12 h at 100 °C, resulting in Cu NCs exhibiting blue PL (excitation at 370 nm and emission at 450 nm), with a PL QY of 9.3%. Huang's group used trypsin as a reducing and stabilizing agent to synthesize Cu NCs under refluxing.[63] As a slight modification of Goswami's method,[54] chicken egg white was used as a template to synthesize Cu Ns,[64] which was mixed with $CuSO_4$ in aqueous solution, followed by the addition of NaOH to promote the reduction of Cu(II) into Cu NCs.

Gao and co-workers designed a bifunctional peptide CCYGGPKKKRKVG as a template to synthesize Cu NCs (Fig. 3B).[65] Excess of NaCl was mixed with Cu(II), forming a coordination complex $CuCl_4^{2-}$, followed by the addition of the peptide, so that the reduction of Cu(II) to Cu(0) occurred under basic conditions (pH = 12). Blue-emitting Cu NCs (excitation at 318 nm and emission at 418 nm) were obtained through ultrafiltration.[65] Huang and co-workers synthesized Cu NCs by the reduction of Cu(II) into Cu(0) by AA, which were clustered onto the peptide CLEDNN.[66] Similar to the results of Ghosh and co-workers,[61] their PL was excitation dependent.

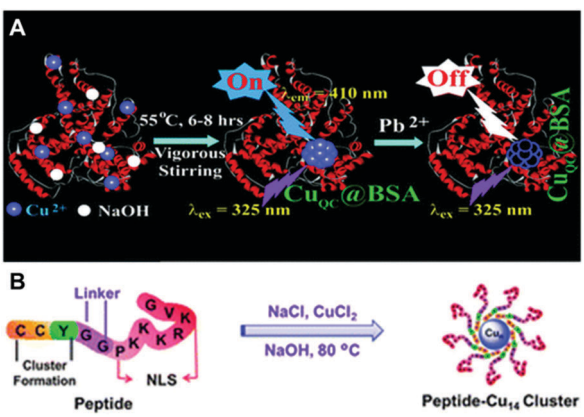

Fig. 3 Schematic illustration for the synthesis of Cu NCs using BSA (A) and a bifunctional peptide (B) as the template. (A) Reproduced with permission from ref. 54, Copyright 2011, American Chemical Society.

2.2. Ligand-assisted methods

Cu NCs are often synthesized with the use of short organic ligands, which contain specific functional chemical groups able to bind with copper. They efficiently prevent clusters from growing into bigger nanoparticles at the synthetic stage, and stabilize them from aggregation by either charge or steric effects. In the following, we sub-divided these kinds of Cu NCs by the nature of chemical groups of the ligands, which are typically thiolate, or carboxyl.

2.2.1 Thiolate ligands. Chen's group synthesized Cu NCs by using 2-mercapto-5-*n*-propylpyrimidine (MPP) as a protecting ligand and $NaBH_4$ as a reducing agent. Copper(II) nitrate and tetra-*n*-octylammonium bromide were co-dissolved in ethanol, followed by cooling in ice water and adding MPP and $NaBH_4$.[9] After centrifugation and purification, clusters with the composition of Cu_8L_4 ($L = C_7H_9N_2S$) were obtained, as was confirmed by the electrospray ionization mass spectrometry (ESI-MS) measurements. This work inspired plenty of use of thiolate-based ligands to synthesize Cu NCs, such as GSH, penicillamine,[67–70] phenylethanethiol,[68] dihydrolipoic acid,[71] mercaptobenzoic acids,[72] cysteamine[73,74] and 3-mercaptotrimethoxysilane.[75] Both the nature of the ligands and the synthetic conditions play an important role in the structure and optical properties of the resulting Cu NCs. Chang's group employed three isomers of mercaptobenzoic acid as ligands to synthesize Cu NCs.[72] Cu NCs protected by 2-mercaptobenzoic acid emitted blue light peaking at 420 nm (excited at 338 nm), with a PL QY of 13.2%. Cu NCs synthesized by using 3-mercaptobenzoic acid and 4-mercaptobenzoic acid tend to form net-like and rod-like aggregates, respectively. Different from the intense blue emission of 2-mercaptobenzoic acid protected Cu NCs, 4-mercaptobenzoic acid protected Cu NCs showed red PL (excitation peak at 324 nm and an emission peak at 646 nm), with a PL QY of only 0.5%, while 3-mercaptobenzoic acid protected Cu NCs showed even weaker red emission with a PL QY of $<0.1\%$.[72] Even using the same ligand may result in different Cu NCs when synthetic conditions change.[76] Wang and co-workers synthesized Cu NCs using GSH as both a reducing agent and a protecting agent.[15] GSH and Cu(II) ions were mixed in aqueous solution with a molar ratio of 4 : 1, forming a white hydrogel owing to the

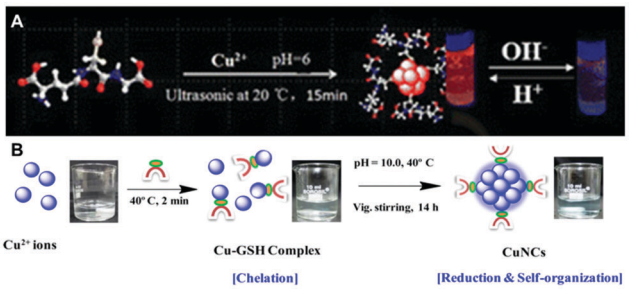

Fig. 4 Schematic illustration for the synthesis of Cu NCs using (A) GSH under ultrasonic treatment, and (B) GSH under heating at 40 °C. (B) Reproduced with permission from ref. 78, Copyright 2015, American Chemical Society.

coordination between Cu(II) ions and GSH. After heating this hydrogel at 80 °C for 10 min and adjusting the pH to 4–5 using NaOH, a light yellow and transparent solution of Cu NCs was obtained, which emitted red PL peaking at 600 nm.[15] Wang *et al.* reported a fast synthetic method towards GSH protected Cu NCs with the aid of ultrasonic treatment, as demonstrated in Fig. 4A.[77] GSH was mixed with Cu(II) ions in aqueous solution, with a molar ratio of 4 : 1, and the pH was adjusted to 6.0 using NaOH, followed by ultrasonic treatment for 15 min. Red-emitting (PL peak at 606 nm) Cu NCs were obtained after purification, which were employed to develop chemical sensors for Pb^{2+}.[77] Mukherjee's group reported GSH protected Cu NCs, but with blue emission (Fig. 4B). In their synthesis, GSH and Cu(II) were mixed in a molar ratio of 1 : 1, forming a complex. The pH of the mixture was adjusted to 10.0 and the precursors were allowed to react for 14 h upon heating at 40 °C, forming Cu clusters with the composition of ($Cu_{15}GSH_4$), which was revealed by matrix assisted laser desorption ionization-time of flight (MALDI-TOF) mass spectrometry analyses.[78] Qian's group synthesized GSH protected Cu NCs in DMF using a one-step method.[79] An aqueous solution of GSH (300 μL, 0.1 M) was mixed with 650 μL DMF followed by the addition of Cu(II) (50 μL, 0.1 M) under vigorous stirring. Immediately, intense orange-red emission could be observed under UV-light, indicating the formation of Cu NCs. TEM images demonstrated that the product of this reaction was composed of aggregates with a size of around 100 nm, consisting of small clusters with a size ranging from 2 to 5 nm. Both our group[80] and Shih's group[81] reported that red-emitting Cu NCs form immediately after mixing GSH and Cu(II) in aqueous solution in a ratio of 5 : 1, with emission peaking at 620 nm (excitation at 365 nm) and a PL QY $<0.1\%$. These Cu NCs experienced aggregation induced emission (AIE) enhancement, with a PL QY improved to as high as 24% after on-purpose aggregation with 95% ethanol.[81]

2.2.2 Carboxyl ligands. Short organic ligands with carboxyl groups were also reported to be capable of protecting Cu NCs. Tannic acid was used to synthesize Cu NCs by reducing Cu(II) using AA, using a one-pot method. Clusters have been obtained showing blue PL emission (emission maximum at 430 nm upon excitation at 360 nm), with a PL QY of 14%.[82] Their blue PL can be efficiently quenched by Fe^{3+} and Eu^{3+}, which has been used to develop metal ion sensors.[82–84] Employing a slightly modified method, sodium cholate[85] and AA[86] were also employed as suitable ligands to protect Cu NCs from aggregation and preserve their PL properties.

2.3. Electrochemical synthesis

In electrochemical synthesis, a sacrificial Cu anode is employed as a copper source. Cu(II) ions are generated by its anodic dissolution, and reduced to Cu NCs which have to be stabilized in solution. In the synthesis reported in 2010 by López-Quintela's group,[87] Cu(II) was generated from a copper sheet (anode) in the presence of 0.1 mol L^{-1} tetrabutylammonium nitrate (supporting electrolyte). Cu_{13} clusters (as confirmed by MALDI-TOF) were obtained, showing reasonably strong blue PL emission (centred at 410 nm) with a PL QY of 13%. Adopting different purification and heat treatments, Cu NCs with different sizes can be achieved.[17] Smaller Cu_5 NCs could be obtained through a purification process by centrifugation in ethanol; larger Cu_{20} NCs were obtained after heating the as-synthesized Cu NCs at 80 °C and re-dissolving them in acetonitrile.[88] The blue emission from Cu_{13} can be quenched by Pb^{2+}, which has been adapted to develop metal ion sensors.[89] More recently, the same group reported the electrochemical synthesis of Cu NCs in pure water avoiding the use of any additional surfactants or ligands[90] by employing extremely small current densities. They had composition of Cu_5, confirmed by ESI-TOF, and showed blue PL emission (with an excitation band at 224 nm and an emission band at 305 nm).

2.4. Etching methods

In an etching method, larger non-luminescent Cu nanoparticles are firstly synthesized, followed by chemical etching in the presence of suitable ligands, resulting in small-sized luminescent Cu NCs. Due to the difference in stability among differently sized clusters, the most robust ones would survive the etching process. Based on this concept, Xie's group synthesized Cu NCs in a mild etching environment made possible by phase transfer *via* electrostatic interactions.[91] Firstly, Cu nanoparticles were synthesized in water by the reduction of Cu(II) using $NaBH_4$, with the protection of GSH. They were transferred to the organic phase (toluene) by adding cetyltrimethylammonium bromide (CTAB), through the electrostatic interaction between the positively charged CTAB and the negatively charged carboxyl groups of GSH on the surface of Cu nanoparticles. After incubation under room temperature for 24 h, blue PL emission (peaked at 438 nm) was observed in the toluene phase, indicating the formation of small sized Cu clusters. Wang's group reported the conversion of non-luminescent Cu nanoparticles to luminescent Cu NCs *via* a size-focusing etching process in aqueous solution.[92] Firstly, Cu nanoparticles were synthesized by the reduction of Cu(II) using AA as both a reducing and protection agent. They were incubated in aqueous solution containing excess GSH, where the size-focusing etching process occurred through a ligand exchange reaction. After 5 h of incubation, Cu NCs were obtained, showing a strong emission peak at 600 nm and a relatively minor emission peak at 426 nm. They also showed the AIE effect, with a PL QY increasing from 0.5% to 6.6% before and

after aggregation, respectively.[92] Other thiol ligands, such as cysteine (Cys)[92,93] and penicillamine,[92] have also successfully been used as etching agents to convert larger copper nanoparticles into luminescent Cu NCs.

2.5. Other methods

López-Quintela's group reported the synthesis of Cu NCs using a microemulsion technique.[94] A water-in-oil microemulsion system was formed after mixing $CuSO_4$ solution (aqueous phase), cyclohexane (oily phase), cyclohexane (oily phase), sodium dodecyl sulfate (surfactant) and isopentanol (co-surfactant). The amount of $NaBH_4$ employed as a reducing agent determined the size of the clusters. Blue emitting Cu NCs with less than 13 atoms in the core were obtained when 0.1 moles of $NaBH_4$ was added, while larger NCs were obtained with an increasing amount of $NaBH_4$ in the system. Kawasaki and co-workers synthesized Cu NCs *via* microwave-assisted polyol synthesis, without using any additional protective and reducing agents.[95]

3. Emission properties of Cu NCs

Different from the large sized metallic Cu nanoparticles, Cu NCs exhibit a discrete electronic structure and molecule-like optical properties. For Cu NCs with a diameter of the metal core typically smaller than 3 nm, the characteristic absorption peak of the larger metal nanoparticles in the range of 500–600 nm originating from the surface plasmonic resonance is not observed.[92] Instead, one or more absorption peaks in the UV or blue wavelength range are commonly recorded, ascribed to the inter-band electronic transitions which are strongly influenced by the nature of the ligands.[14,16] The PL properties of small sized Cu nanoparticles have been reported by Siwach and co-workers and very weak PL emission peaking at 296 nm when excited in the range of 200–240 or 250–280 nm was observed.[96] They attributed the PL to electronic transitions from excited states to 3d levels. In one of the early reports on Cu NCs synthesized by a microemulsion technique, López-Quintela's group reported their blue PL emission.[94] Afterwards, different PL emission colours have been mentioned for different Cu NCs, such as blue, green, orange, or red. The origin of this emission and the key factors determining the PL QY and the emission colour are still under investigations. In the following sub-sections, we will discuss this in relation to the metal cores, ligands, and environment.

3.1. The effect of the metal core

At the beginning of the research on Cu NCs, their PL was supposed to originate from the quantum confinement similar to that occurring for semiconductor quantum dots, with an assumption that the emission would shift to longer wavelengths with increasing cluster size. The simple spherical Jellium model, initially employed to describe the emission energy of Au NCs, was adapted to represent the relationship between the emission energy of Cu NCs and their size through the expression: $E_g = E_{fermi}/N^{1/3}$, where E_g is the emission energy of clusters, E_{fermi} is the Fermi energy of the bulk metal and N is the number of atoms in single clusters. We summarized the size of Cu NCs (measured by mass spectrometry) and their PL properties reported in the literature in Table 1. Some Cu NCs followed the Jellium model expression indeed, such as Cu NCs stabilized by tetrabutylammonium salt showing PL emission peaked at 410 nm (3.02 eV) for the composition of less than 14 copper atoms.[87] Cu NCs with a metal core of Cu_5, Cu_{13}, and Cu_{20} stabilized by tetrabutylammonium salt showed PL emission peaking at 305 nm (4.07 eV), 425 nm (2.92 eV) and 500 nm (2.48 eV), respectively.[17] Cu NCs stabilized by BSA showed PL emission peaking at 410 nm, consistent with the presence of Cu_{13} as estimated from the MALDI-TOF analysis. The composition of blue emitting (PL at 430 nm, or 2.88 eV) Cu NCs stabilized by GSH was measured to be Cu_{15} by MALDI-TOF, which was very close to the calculated number of atoms in the core (14.6) by a spherical Jellium model.[78] The composition of non-protected Cu NCs, with an emission peaking at 305 nm (4.07 eV), was measured to be Cu_5 by ESI-TOF, which is the same as the calculated number.[90] However, for a considerable number of other Cu NCs such as those stabilized by poly(methacrylic acid),[20] PVP/dihydrolipoic acid,[28] mercaptobenzoic acids,[72] and penicillamine[67] the Jellium model did not fit the size measured by mass spectrometry. It seems that the Jellium model is better suited for non-protected clusters, or those protected by weakly bound ligands, or bigger sized Cu NCs (no less than 5 atoms in a single cluster) which typically show UV or blue PL emission with a relatively short PL lifetime of several nanoseconds ascribed to singlet excited states of the metal core.[92] For the Cu NCs stabilized by strongly bound ligands (thiolate for example) or small sized clusters ($\leq$3 Cu atoms in a single cluster), the Jellium model failed to describe the relationship between the emission energy and the size of the Cu core. Those Cu NCs usually showed PL in the orange-red spectral range, with a relatively long PL lifetime of several to a hundred μs, which is supposed to originate from the Cu(I)–ligand complex condensing on the surface of the Cu(0) core,[82] through ligand-to-metal charge transfer from the Cu(I)–ligand complex to the Cu atoms in the core, followed by radiative relaxation through a metal-centered triplet state. This is supported by the report on Cu NCs with dual emission (around 420 nm and 600 nm), where the blue emission peak showed a short PL lifetime of several ns and the orange-red peak – in the range of μs.[92] Also the presence of Cu(I) is critical for PL, confirmed by the results that a strong decrease of PL intensity was observed after further reduction of luminescent Cu NCs with $NaBH_4$.[73]

Overall, the key factors determining the emission color of the Cu NCs are still rather contradictory. As demonstrated in Table 1 (representative examples of Cu NCs stabilized by different ligands), the core size is indeed not the only factor to determine their emission color. In the next two sub-sections, we will show that the nature of the ligands, and the environment of Cu NCs also play a role in this respect. Also, for subnanometer-sized metal clusters, conventional (even high-resolution) TEM studies are not necessarily a reliable technique in the evaluation of cluster size.

Table 1 Representative examples of Cu NCs stabilized by different ligands, giving the number of Cu atoms in the metal core, PLE and PL peak positions, and PL QY. In cases where the symbol "—" is used, no relevant data are provided in the respective literature

Size	Protection ligand	PLE	PL	Lifetime	QY (%)	Ref.
Cu_5	Poly(methacrylic acid)	360	630	—	2.2	20
—	Polyetherimide	355	430	—	2.1	24
Cu_6	Poly(acrylic acid) *graft*-mercaptoethylamine	365	630	—	5.7	21
Cu_4	PVP/dihydrolipoic acid	365	435, 650	0.8 μs	10.8	28
—	dsDNA	344	593	3.54 μs	—	33
Cu_5	BSA	365	410	—	—	97
$Cu_{5,13}$	BSA	325	410	0.4 ns	15	54
—	BSA	320	420	—	—	55
Cu_{12}	Human serum albumin	330	414	2.7 ns	4	98
—	Lysozyme	365	600	—	5.6	99
$Cu_{2,4,9}$	Lysozyme	360	450	6.5 ns	18	61
—	Papain	370	620	—	14.3	60
—	Trypsin	363	455	4.6 ns	1.1	56
—	Transferrin	508	670	15.2 ns	6.2	100
—	Yeast extract	370	450	16.2 ns	9.3	62
—	Chicken egg white	337	417	3.9 ns	0.98	64
Cu_{14}	Peptide	318	418	—	—	65
—	Peptide	373	454	—	7.3	66
$Cu_{2,3,4,5}$	GSH	340	627	15.2 μs	1.9	79
$Cu_{3,4}$	GSH	340	620	—	3	81
$Cu_{1,2,3}$	GSH	410	610	—	5	15
—	GSH	360	600	—	3.6	76
Cu_{15}	GSH	340	430	2.7 ns	6	78
$Cu_{1,2}$	GSH	345	620	—	—	92
$Cu_{4,5,6}$	D-Penicillamine	345	418, 640	1.8 ns 150 μs	16.6	67
$Cu_{1,2}$	Penicillamine	326	580	126.5 ns	2	69
—	Cysteine	365	490	9.6 ns	8.8	74
Cu_4	Cysteine	375	480	—	—	101
—	Cysteine	360	490	—	5.6	73
Cu_{38}	Phenylethanethiol	405	605	—	—	68
—	2-Mercaptobenzoic acid	338	420	6.5 ns	13.2	72
—	AA	370	454	2.4 ns	—	86
—	Tannic acid	360	425	1.4 ns	—	83
$Cu_{3,4,5,6}$	Histidine	350	456	—	1.6	102
—	Tannic acid	355	430	1.8 ns		84
$Cu_{12,13}$	Tetrabutylammonium nitrate	300	410	—	13	87
Cu_5	Non-protected	224	305	—	—	90
Cu_9	Non-protected	350	475	—	0.65	95

3.2. The effect of surface ligands

Surface ligands play an important role in the optical properties of Cu NCs, especially for the PL QY. For the majority of Cu NCs summarized in Table 1, their QY is still relatively low, usually around 10%. For those reported Cu NCs whose QY exceeded 10%, most of them were stabilized by proteins or polymers containing many electron-rich groups, such as –COOH, $–NH_2$, or –OH. The effect of such electron-rich groups on ligands is systematically addressed in ref. 30. Cysteine, cysteamine, mercaptoethanol and mercaptopropionic acid, all thiols which are similar in structure but with varying end-chemical groups, were used for post-preparative treatment of PVP-supported Cu NCs. As a result of this treatment, the PL QY followed the order of cysteine > cysteamine > mercaptoethanol > mercaptopropionic acid, corresponding to the electron donation ability of the end-chemical groups. This confirmed that the electron-rich groups of the ligands indeed improve the PL QY of Cu NCs, similar to that of Au and Ag cases.[103]

3.3. The effect of environment

3.3.1 Effect of solvents. López-Quintela's group systematically compared PL spectra of tetrabutylammonium nitrate stabilized Cu NCs in different solvents (water, pentane, chloroform, and ethanol).[87] Compared with the spectrum of Cu NCs in water (single peak at 400 nm), the samples showed additional vibronic peaks at 385, 406, and 428 nm in lower polarity solvents, and an increase of the Stokes shift of the main PL peak with the increasing polarity of the solvent was also observed. Ling and co-workers systematically studied the solvent effect on the PEI protected Cu NCs,[104] dispersing them into 12 kinds of organic solvents (Fig. 5A). The PL QYs of Cu NCs dispersed in all those solvents were higher than that in water, with the highest PL QY of 21% in THF. PL emission peaks in alcohols (methanol, ethanol, ispropanol, *n*-propanol, ethylene glycol and *n*-butyl alcohol), acetonitrile, and DMSO were the same like in the original aqueous solution. A blue shift of the PL peak was observed in THF and 1,4-dioxane, which was explained by their stronger ability to form hydrogen bonds leading to an increase of the separation between the energy levels of the clusters.

3.3.2 Effect of aggregation. Cu NCs in solution are rather easy to aggregate, as a result of disturbing the surface charge or destroying the template structure. Aggregation of light emitting samples often causes PL quenching, typically related to the

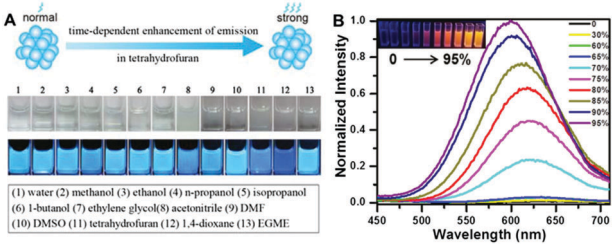

Fig. 5 (A) Solvent effect on PEI protected Cu NCs; (B) PL emission spectra (excited at 365 nm) of Cu NCs in the mixture of water and ethanol with different percentages of ethanol (noted on the frame); inset picture presents a photograph of the respective solution under UV light, demonstrating their increasing emission intensity due to the AIE effect. (A) Reproduced with permission from ref. 105, Copyright 2015, American Chemical Society.

non-radiative Förster resonant energy transfer to the neighboring close-packed nanoparticles with lower PL QY.[105] On the other hand, the aggregation-induced emission (AIE) phenomenon has been discovered by Tang's group for the organic molecules of 1-methyl-1,2,3,4,5-pentaphenylsilole, which is a useful approach to achieve high PL QY.[106] Cu NCs stabilized by thiol ligands were reported to possess AIE properties, also[79–81,92,93,107,108] leading to more than 10-fold enhancement of the PL QY.

Their AIE has been ascribed to the restriction of intramolecular motion in the aggregation states, which activated the radiative decay and blocked the nonradioactive path, resulting in a higher PL QY of the clusters.[109] Jia and co-workers reported the AIE properties of Cu NCs obtained by ligand etching methods.[92] Their as-synthesized Cu NCs had a weak red PL emission (peaked at 620 nm), while an enhancement of the PL intensity (PL QY from 0.5% to 6.6%) and a blue shift of the emission peak were observed upon ethanol induced aggregation. Our group demonstrated an AIE on chemically synthesised, GSH protected Cu NCs.[80] Similar to Jia and coworker's results, enhanced PL QY and a blue shift of the PL peak were observed upon ethanol induced aggregation, as shown in Fig. 5B. Aggregated Cu NCs formed uniform quasi-spherical agglomerates (50 nm in diameter) with small Cu NCs (<2 nm) inside and a PL QY as high as 24%. D-Penicillamine[107] and cysteine[93] protected Cu NCs also possessed AIE properties.

3.4. Stability of Cu NCs

The stability of Cu NCs is a key concern for their practical applications. Rather often, Cu NCs were reported to suffer from issues of aggregation and/or oxidation, accompanied by the quenching of their PL, which is related to their extremely small size and easy oxidation of Cu (E^0, 0.34 V).[61] The aggregation of clusters is driven by their high surface energy, caused by the high surface/volume ratio. Coating Cu NCs with a protective shell of capping ligands commonly helps in avoiding their aggregation and oxidation. Cu NCs capped by poly(ethylene glycol) showed long-term stability (more than 2 months) without decreasing the PL intensity in a broad pH range (3 to 12).[69] PEI coated Cu NCs presented high stability toward the ambient environment, and no change of the PL intensity was observed after dispersing them into 100 mM NaCl solution. For the PVP-supported Cu NCs additionally treated with citrate,[24] only a minor difference of the PL intensity was recorded (<10% decrease) after 1 month of storage, which was in strong contrast to the similar but non-treated samples.[30]

4. Applications of luminescent Cu NCs

The synthetic advances have enabled the fabrication of stable and reasonably strongly luminescent Cu NCs. Compared with other common fluorophores, such as semiconductor quantum dots, polymer dots and organic dyes, Cu NCs offer several advantages, including molecular-like optical properties, low or no toxicity, high photostability, and large Stokes shifts.[1,110,111] Importantly, Cu is a chemical element which is abundant, inexpensive, and readily available from commercial sources. Recently, Cu NCs have been considered for several applications such as chemical sensors, biological imaging, and light emitting devices (LEDs). In this section, we review applications of luminescent Cu NCs in biological imaging and optoelectronic devices, since two recent reviews[10,12] have already addressed their use in the chemical sensor field. Note however that in the previous synthetic sections we mentioned the use of the respective NCs for developing chemical and metal ion sensors, wherever relevant.

4.1. Biological imaging

The features of small size, low toxicity, and variable surface chemistry provided by different ligands, and reasonably strong PL QY make Cu NCs suitable candidates as fluorophores for biological imaging. In particular, Cu NCs stabilized by proteins, peptides, DNA, or short ligands with functional chemical groups are promising. A good example of such functionalization is blue emitting (peaked at 450 nm), lysozyme protected Cu NCs with a PL QY of 18%, which have been used for the fluorescence labelling of HeLa cells (as shown in Fig. 6A).[61] Similarly, blue emitting Cu NCs functionalized with peptides[66] (with the amino acid sequence CLEDNN) and PEI[112] were employed for labelling of HeLa cells and 293T cells, respectively. Mukherjee's group carried out a cell viability study and uptake assays of blue emitting GSH capped Cu NCs on three different cancerous cell lines, including HeLa (malignant immortal cell line derived from cervical cancer), A549 (human lung carcinoma) and MDAMB-231 (human breast adenocarcinoma).[78] Using laser scanning confocal microscopy, they found that Cu NCs tended to localize in the region surrounding the nucleus. Cao and co-workers used blue emitting Cu NCs (peaked at 430 nm) stabilized by tannic acid for imaging ferric ions in A549 cells.[82]

For the blue emitting Cu NCs, UV excitation lasers have to be employed, so issues such as auto-fluorescence of bio-tissues and the light damage of the cells caused by UV lasers are matters of concern. To avoid such problems, red emitting Cu NCs which can be excited by lower energy light have been employed. Zhang's group used BSA protected red emitting Cu NCs (emission peaked at 625 nm when excited at 524 nm) as a

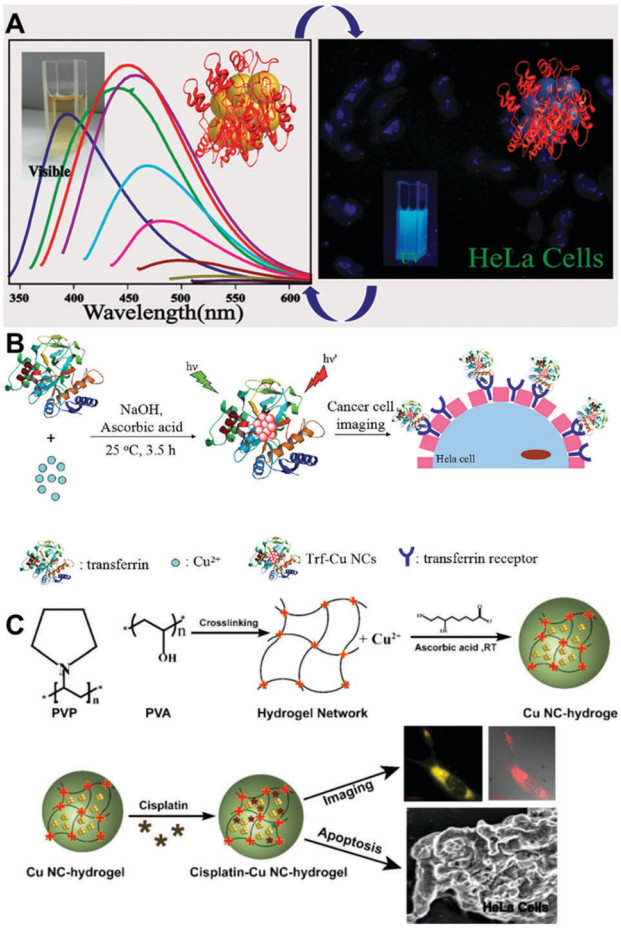

Fig. 6 (A) PL spectra of lysozyme protected Cu NCs (left) and their fluorescence images in HeLa cells. (B) Schematic illustration of the synthesis and cell imaging of transferrin protected Cu NCs. (C) Schematic illustration of the synthesis and cell imaging of hydrogel network protected Cu NCs. (A) Reproduced with permission from ref. 61, Copyright 2014, American Chemical Society. (C) Reproduced with permission from ref. 28, Copyright 2015, American Chemical Society.

probe for cellular imaging.[56] Bhamore and co-workers reported multicolor imaging (blue when excited at 405 nm and green when excited at 488 nm) in *Bacillus subtilis* cells, based on the excitation dependent emission properties of egg white protected Cu NCs.[113] Red emitting GSH protected Cu NCs, quenched by Pb^{2+} ions or high temperature, were applied for sensing those ions and the temperature in CAL-27 cells and MC3T3-E1 cells, respectively. Barthel and co-workers studied the cellular uptake of PEG protected red emitting Cu NCs (emission peaked at 580 nm, excited at 500 nm),[14] localizing them in the cell nuclei area. Zhao and co-workers used transferrin protected red emitting Cu NCs for targeted imaging of HeLa and 3T3 cells, achieving selective imaging of transferrin over-expressed cancer cells, as shown in Fig. 6B.[100] Ghosh and co-workers synthesized a hydrogel through cross-linking PVP protected Cu NCs with poly(vinyl alcohol), and used it to deliver an anticancer drug (cisplatin) and induce the apoptotic death of cells with simultaneous imaging (Fig. 6C).[28]

4.2. Light-emitting devices (LEDs)

Due to the features of long-lifetime, energy-saving and high luminous efficiency, LEDs are considered to be useful alternatives for conventional incandescent lamps.[1,114] Among the white colour LEDs, down-conversion devices employing single or multiple phosphors excited by blue or UV LED chips, are the most popular configuration.[115] Phosphors are down-conversion materials able to generate light with controllable colours, which can be combined together and generate white light with different shades following the RGB concept (R = red; G = green; B = blue). Most of the commercial phosphors employed in LEDs nowadays are based on rare-earth elements, such as terbium, europium and yttrium.[116] The advantages of rare-earth based phosphors are high stability and high PL QY. However, their supply is facing a serious shortage, and the lack of recycling ability is destructive to the environment. Copper is a cheap, earth abundant element, so Cu NCs are increasingly getting attention as phosphors for LEDs. Yang's group fabricated white LEDs combining blue-green emitting Cu ribbons, yellow emitting Cu nanosheets and red emitting Au nanosheets with UV LED chips, achieving Commission Internationale de l'Eclairage (CIE) color coordinates of (0.32, 0.36).[108] The Cu ribbons and nanosheets were assembled from dibenzyl ether protected Cu NCs, and showed AIE properties. Our group reported on white LEDs combining blue emitting Cu NCs with green and red emitting commercial phosphors deposited on a UV LED chip, with CIE coordinates and a colour rendering index (CRI) of (0.35, 0.33) and 92, respectively.[30] The CRI is an index characterizing the light's ability to show object colours naturally compared to daylight (with the maximum value equal to 100). The blue emitting Cu NCs were synthesized by using PVP as the template and post-treated by GSH, resulting in a high PL QY of 27%. Due to the efficient protection by the PVP template, no decrease of their PL QY was observed in the powdered state. We further developed all-Cu NC based white LEDs by combining blue emitting and orange emitting Cu NCs, avoiding the use of rare-earth or noble metal materials, as shown in Fig. 7A.[80] The orange emitting Cu NCs were protected by GSH, and showed AIE properties achieving PL QY as high as 43% in the solid state. They also presented a relatively wide

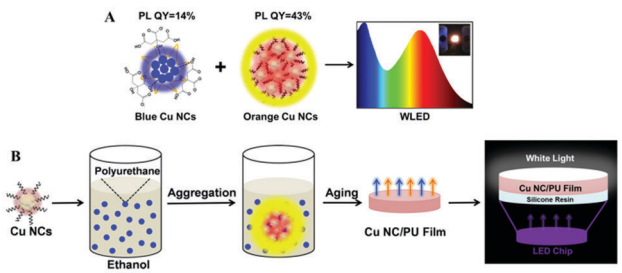

Fig. 7 (A) Schematic illustration of the fabrication of white LEDs based on blue and orange emitting Cu NCs. The inset in the right frame shows a photograph of the working LED. (B) Schematic illustration of the synthesis of dual emission Cu NC/PU films and their use for remote LEDs. (B) Reproduced with permission from ref. 118, Copyright 2016, American Chemical Society.

emission spectrum, leading to the high CRI of fabricated white LEDs. In addition, a large Stoke shift (more than 200 nm) and the absence of any absorption peaks in the blue to green spectral range for orange emitting Cu NCs resulted in a minor overlap between the emission of blue emitting Cu NCs and the absorption of orange Cu NCs, ensuring high colour stability of the resulting white LEDs.

Other issues for down-conversion LEDs are how to decrease the operating temperature of the LED chip and avoid the effect of the packing resin on the color quality of the embedded phosphors. A remote phosphor configuration of white LEDs, a technology which spatially separates the light emitting phosphors from the LED chip used for their excitation, can effectively solve those problems. Liu and co-authors fabricated remote white LEDs employing Cu NC and Au NC films fixed onto ITO glass by electrophoretic deposition.[117] We followed the concept of the remote white LED by using dual emission (orange from Cu NCs and blue from the light emitting polymer) composite films of aggregated Cu NCs in polyurethane, as shown in Fig. 7B.[118] Composite Cu NC@polyurethane films were free-standing and stretchable, and showed thermally stable emission with an overall PL QY of 18%, resulting in remote white LEDs with CIE colour coordinates and a CRI of (0.34, 0.29) and 87, respectively.

5. Conclusions and outlook

This review summarized recent progress in Cu NCs, including their wet chemical synthesis methods, studies of the PL mechanism, and applications related to their emission of light, such as chemical/ion metal sensing, biological imaging and light emitting devices. Several useful features such as earth abundance, low price, ease of synthesis and light emission tunable over the whole visible spectral range, make Cu NC related research a burgeoning field. As surface protecting templates/ligands play an important role in the stability and properties of Cu NCs, their wet chemical synthetic methods are naturally classified by the nature of the capping agents. The optical properties of Cu NCs are influenced by the size (number of Cu atoms) of the metal core, the surface ligands, and the environment. Overall improvements of PL emission stability and further enhancements of the PL QY of Cu NCs are still in focus for subsequent developments.

In spite of the impressive progress in all the areas related to Cu NCs, there are still several challenges to be addressed. Similar to Au or Ag NCs, the origin of PL and the key factors determining the PL QY and the emission colours of the clusters are still under debate. To derive a clear picture behind the PL mechanisms, the exact determination of the crystal structure of Cu NCs, including the arrangement of metal atoms and metal–ligand bonding would be an important step forward, which has been a difficult task for a while due to their easy oxidation. Only recently, several publications reported the single crystal analysis of Cu NCs,[10,119] but the in-depth discussion on the relationships between their structure and optical properties is still a matter of forthcoming studies.

A useful property of Cu NCs is the ability to significantly improve their emission by the aggregation induced effect, which has already been utilized in optoelectronic applications.[118] To achieve the AIE effect, solvent induced controlled aggregation of Cu NCs is commonly employed, often rendering the resulting cluster aggregates less stable in biological environments. The forthcoming improvements and refinements of this approach would help to provide brightly emitting Cu NCs for biological applications, such as bio-imaging and drug delivery. The availability of red emitting Cu NCs with high PL QY which can be excited in the visible instead of the UV region is required for imaging applications.

Yet another promising application of Cu NCs is in down-conversion colourful and white LEDs, where they are used in emitting layers as earth abundant, non-toxic and rather cheap phosphors. Potential commercialization of Cu NCs for LEDs will require further improvements in both their long-term stability and the efficiency of the resulting devices.

Acknowledgements

This work was supported by the Research Grant Council of Hong Kong S.A.R. (project T23-713/11), The Hong Kong Scholar Program (XJ2014046), the Natural Science Foundation of Youth Fund Project of China (51602024) and China Postdoctoral Science Foundation (2014M550621).

Notes and references

1 Y. Tao, M. Li, J. Ren and X. Qu, *Chem. Soc. Rev.*, 2015, **44**, 8636–8663.
2 J. P. Wilcoxon and B. L. Abrams, *Chem. Soc. Rev.*, 2006, **35**, 1162–1194.
3 L. Zhang and E. Wang, *Nano Today*, 2014, **9**, 132–157.
4 M. Turner, V. B. Golovko, O. P. H. Vaughan, P. Abdulkin, A. Berenguer-Murcia, M. S. Tikhov, B. F. G. Johnson and R. M. Lambert, *Nature*, 2008, **454**, 981–983.
5 Y. Negishi, K. Nobusada and T. Tsukuda, *J. Am. Chem. Soc.*, 2005, **127**, 5261–5270.
6 C. P. Joshi, M. S. Bootharaju and O. M. Bakr, *J. Phys. Chem. Lett.*, 2015, **6**, 3023–3035.
7 A. S. Susha, M. Ringler, A. Ohlinger, M. Paderi, N. LiPira, G. Carotenuto, A. L. Rogach and J. Feldmann, *Chem. Mater.*, 2008, **20**, 6169–6175.
8 R. Jin, *Nanoscale*, 2015, **7**, 1549–1565.
9 W. Wei, Y. Lu, W. Chen and S. Chen, *J. Am. Chem. Soc.*, 2011, **133**, 2060–2063.
10 Y. Guo, F. Cao, X. Lei, L. Mang, S. Cheng and J. Song, *Nanoscale*, 2016, **8**, 4852–4863.
11 Y. Lu, W. Wei and W. Chen, *Chin. Sci. Bull.*, 2012, **57**, 41–47.
12 X. Hu, T. Liu, Y. Zhuang, W. Wang, Y. Li, W. Fan and Y. Huang, *Trends Anal. Chem.*, 2016, **77**, 66–75.
13 Z. Qing, X. He, D. He, K. Wang, F. Xu, T. Qing and X. Yang, *Angew. Chem., Int. Ed.*, 2013, **125**, 9901–9904.

14 M. J. Barthel, I. Angeloni, A. Petrelli, T. Avellini, A. Scarpellini, G. Bertoni, A. Armirotti, I. Moreels and T. Pellegrino, *ACS Nano*, 2015, **9**, 11886–11897.
15 C. Wang, L. Ling, Y. Yao and Q. Song, *Nano Res.*, 2015, **8**, 1975–1986.
16 M. Zhao, L. Sun and R. M. Crooks, *J. Am. Chem. Soc.*, 1998, **120**, 4877–4878.
17 N. Vilar-Vidal, J. Rivas and M. A. López-Quintela, *ACS Catal.*, 2012, **2**, 1693–1697.
18 L. Balogh and D. A. Tomalia, *J. Am. Chem. Soc.*, 1998, **120**, 7355–7356.
19 P. N. Floriano, C. O. Noble, IV, J. M. Schoonmaker, E. D. Poliakoff and R. L. McCarley, *J. Am. Chem. Soc.*, 2001, **123**, 10545–10553.
20 H. Zhang, X. Huang, L. Li, G. Zhang, I. Hussain, Z. Li and B. Tan, *Chem. Commun.*, 2012, **48**, 567–569.
21 R. Gui, J. Sun, X. Cao, Y. Wang and H. Jin, *RSC Adv.*, 2014, **4**, 29083–29088.
22 F.-U. Mónica, T.-A. Laura, M. C.-F. José, P. Rosario and S.-M. Alfredo, *Nanotechnology*, 2013, **24**, 495601.
23 Y. Ling, N. Zhang, F. Qu, T. Wen, Z. F. Gao, N. B. Li and H. Q. Luo, *Spectrochim. Acta, Part A*, 2014, **118**, 315–320.
24 J. Feng, Y. Ju, J. Liu, H. Zhang and X. Chen, *Anal. Chim. Acta*, 2015, **854**, 153–160.
25 Z.-C. Liu, J.-W. Qi, C. Hu, L. Zhang, W. Song, R.-P. Liang and J.-D. Qiu, *Anal. Chim. Acta*, 2015, **895**, 95–103.
26 Y. Zhong, Q. Wang, Y. He, Y. Ge and G. Song, *Sens. Actuators, B*, 2015, **209**, 147–153.
27 Y. Ling, J. X. Li, F. Qu, N. B. Li and H. Q. Luo, *Microchim. Acta*, 2014, **181**, 1069–1075.
28 R. Ghosh, U. Goswami, S. S. Ghosh, A. Paul and A. Chattopadhyay, *ACS Appl. Mater. Interfaces*, 2015, **7**, 209–222.
29 Q. Tang, T. Yang and Y. Huang, *Microchim. Acta*, 2015, **182**, 2337–2343.
30 Z. Wang, A. S. Susha, B. Chen, C. Reckmeier, O. Tomanec, R. Zboril, H. Zhong and A. L. Rogach, *Nanoscale*, 2016, **8**, 7197–7202.
31 A. Rotaru, S. Dutta, E. Jentzsch, K. Gothelf and A. Mokhir, *Angew. Chem., Int. Ed.*, 2010, **49**, 5665–5667.
32 Q. Song, Y. Shi, D. He, S. Xu and J. Ouyang, *Chem. – Eur. J.*, 2015, **21**, 2417–2422.
33 X. Jia, J. Li, L. Han, J. Ren, X. Yang and E. Wang, *ACS Nano*, 2012, **6**, 3311–3317.
34 C.-A. Chen, C.-C. Wang, Y.-J. Jong and S.-M. Wu, *Anal. Chem.*, 2015, **87**, 6228–6232.
35 C. Song, X. Yang, K. Wang, Q. Wang, J. Huang, J. Liu, W. Liu and P. Liu, *Anal. Chim. Acta*, 2014, **827**, 74–79.
36 Z. Zhou, Y. Du and S. Dong, *Anal. Chem.*, 2011, **83**, 5122–5127.
37 R. Hu, Y.-R. Liu, R.-M. Kong, M. J. Donovan, X.-B. Zhang, W. Tan, G.-L. Shen and R.-Q. Yu, *Biosens. Bioelectron.*, 2013, **42**, 31–35.
38 J. Chen, J. Liu, Z. Fang and L. Zeng, *Chem. Commun.*, 2012, **48**, 1057–1059.
39 J. Liu, J. Chen, Z. Fang and L. Zeng, *Analyst*, 2012, **137**, 5502–5505.
40 Y. Hu, Y. Wu, T. Chen, X. Chu and R. Yu, *Anal. Methods*, 2013, **5**, 3577–3581.
41 Y.-R. Liu, R. Hu, T. Liu, X.-B. Zhang, W. Tan, G.-L. Shen and R.-Q. Yu, *Talanta*, 2013, **107**, 402–407.
42 H.-B. Wang, H.-D. Zhang, Y. Chen and Y.-M. Liu, *New J. Chem.*, 2015, **39**, 8896–8900.
43 L. Zhang, J. Zhao, M. Duan, H. Zhang, J. Jiang and R. Yu, *Anal. Chem.*, 2013, **85**, 3797–3801.
44 L. Zhang, J. Zhao, H. Zhang, J. Jiang and R. Yu, *Biosens. Bioelectron.*, 2013, **44**, 6–9.
45 F. Xu, H. Shi, X. He, K. Wang, D. He, Q. Guo, Z. Qing, L. a. Yan, X. Ye, D. Li and J. Tang, *Anal. Chem.*, 2014, **86**, 6976–6982.
46 X.-P. Wang, B.-C. Yin and B.-C. Ye, *RSC Adv.*, 2013, **3**, 8633–8636.
47 Z. Qing, T. Qing, Z. Mao, X. He, K. Wang, Z. Zou, H. Shi and D. He, *Chem. Commun.*, 2014, **50**, 12746–12748.
48 L. Guiying, S. Yong, P. Jian, D. Wei, L. Lingling, X. Shujuan, W. Fei and W. Xiaohua, *Nanotechnology*, 2013, **24**, 345502.
49 Z. Qing, X. He, T. Qing, K. Wang, H. Shi, D. He, Z. Zou, L. Yan, F. Xu, X. Ye and Z. Mao, *Anal. Chem.*, 2013, **85**, 12138–12143.
50 C. Wu, C. Zhou, E. Wang and S. Dong, *Nanoscale*, 2016, **8**, 14243–14249.
51 B.-Z. Chi, R.-P. Liang, W.-B. Qiu, Y.-H. Yuan and J.-D. Qiu, *Biosens. Bioelectron.*, 2017, **87**, 216–221.
52 S.-S. Zhou, L. Zhang, Q.-Y. Cai, Z.-Z. Dong, X. Geng, J. Ge and Z.-H. Li, *Anal. Bioanal. Chem.*, 2016, 1–7.
53 H.-W. Zhu, W.-X. Dai, X.-D. Yu, J.-J. Xu and H.-Y. Chen, *Talanta*, 2015, **144**, 642–647.
54 N. Goswami, A. Giri, M. S. Bootharaju, P. L. Xavier, T. Pradeep and S. K. Pal, *Anal. Chem.*, 2011, **83**, 9676–9680.
55 X. Liao, R. Li, Z. Li, X. Sun, Z. Wang and J. Liu, *New J. Chem.*, 2015, **39**, 5240–5248.
56 C. Wang, C. Wang, L. Xu, H. Cheng, Q. Lin and C. Zhang, *Nanoscale*, 2014, **6**, 1775–1781.
57 Y. Zhong, J. Zhu, Q. Wang, Y. He, Y. Ge and C. Song, *Microchim. Acta*, 2015, **182**, 909–915.
58 X. Deng, X. Huang and D. Wu, *Anal. Bioanal. Chem.*, 2015, **407**, 4607–4613.
59 L. Hu, Y. Yuan, L. Zhang, J. Zhao, S. Majeed and G. Xu, *Anal. Chim. Acta*, 2013, **762**, 83–86.
60 H. Miao, D. Zhong, Z. Zhou and X. Yang, *Nanoscale*, 2015, **7**, 19066–19072.
61 R. Ghosh, A. K. Sahoo, S. S. Ghosh, A. Paul and A. Chattopadhyay, *ACS Appl. Mater. Interfaces*, 2014, **6**, 3822–3828.
62 L. Jin, Z. Zhang, A. Tang, C. Li and Y. Shen, *Biosens. Bioelectron.*, 2016, **79**, 108–113.
63 W. Wang, F. Leng, L. Zhan, Y. Chang, X. X. Yang, J. Lan and C. Z. Huang, *Analyst*, 2014, **139**, 2990–2993.
64 Y. Qiao, T. Xu, Y. Zhang, C. Zhang, L. Shi, G. Zhang, S. Shuang and C. Dong, *Sens. Actuators, B*, 2015, **220**, 1064–1069.
65 Y. Wang, Y. Cui, R. Liu, Y. Wei, X. Jiang, H. Zhu, L. Gao, Y. Zhao, Z. Chai and X. Gao, *Chem. Commun.*, 2013, **49**, 10724–10726.

66 H. Huang, H. Li, A.-J. Wang, S.-X. Zhong, K.-M. Fang and J.-J. Feng, *Analyst*, 2014, **139**, 6536–6541.
67 X. Jia, X. Yang, J. Li, D. Li and E. Wang, *Chem. Commun.*, 2014, **50**, 237–239.
68 A. Ganguly, I. Chakraborty, T. Udayabhaskararao and T. Pradeep, *J. Nanopart. Res.*, 2013, **15**, 1–7.
69 M. Jia-Ying, C. Po-Cheng and C. Huan-Tsung, *Nanotechnology*, 2014, **25**, 195502.
70 S. M. Lin, S. Geng, N. Li, N. B. Li and H. Q. Luo, *Talanta*, 2016, **151**, 106–113.
71 T. Zhou, Q. Yao, T. Zhao and X. Chen, *Talanta*, 2015, **141**, 80–85.
72 Y.-J. Lin, P.-C. Chen, Z. Yuan, J.-Y. Ma and H.-T. Chang, *Chem. Commun.*, 2015, **51**, 11983–11986.
73 M. Cui, G. Song, C. Wang and Q. Song, *Microchim. Acta*, 2015, **182**, 1371–1377.
74 Z. Tingyao, X. Wei, Y. Qiuhong, Z. Tingting and C. Xi, *Methods Appl. Fluoresc.*, 2015, **3**, 044002.
75 S. Zhou, Y. Li, F. Wang and C. Wang, *RSC Adv.*, 2016, **6**, 38897–38905.
76 Y. Luo, H. Miao and X. Yang, *Talanta*, 2015, **144**, 488–495.
77 C. Wang, H. Cheng, Y. Huang, Z. Xu, H. Lin and C. Zhang, *Analyst*, 2015, **140**, 5634–5639.
78 N. K. Das, S. Ghosh, A. Priya, S. Datta and S. Mukherjee, *J. Phys. Chem. C*, 2015, **119**, 24657–24664.
79 Y. Huang, W. Liu, H. Feng, Y. Ye, C. Tang, H. Ao, M. Zhao, G. Chen, J. Chen and Z. Qian, *Anal. Chem.*, 2016, **88**, 7429–7434.
80 Z. Wang, B. Chen, A. S. Susha, W. Wang, C. J. Reckmeier, R. Chen, H. Zhong and A. L. Rogach, *Adv. Sci.*, 2016, **3**, 1600182.
81 J. Liu, Q. M. Zhang, Y. Feng, Z. Zhou and K. Shih, *ChemPhysChem*, 2016, **17**, 225–231.
82 H. Cao, Z. Chen, H. Zheng and Y. Huang, *Biosens. Bioelectron.*, 2014, **62**, 189–195.
83 H. Cao, Z. Chen and Y. Huang, *Talanta*, 2015, **143**, 450–456.
84 H. Rao, H. Ge, Z. Lu, W. Liu, Z. Chen, Z. Zhang, X. Wang, P. Zou, Y. Wang, H. He and X. Zeng, *Microchim. Acta*, 2016, **183**, 1651–1657.
85 J.-S. Shen, Y.-L. Chen, Q.-P. Wang, T. Yu, X.-Y. Huang, Y. Yang and H.-W. Zhang, *J. Mater. Chem. C*, 2013, **1**, 2092–2096.
86 X.-J. Zheng, R.-P. Liang, Z.-J. Li, L. Zhang and J.-D. Qiu, *Sens. Actuators, B*, 2016, **230**, 314–319.
87 N. Vilar-Vidal, M. C. Blanco, M. A. López-Quintela, J. Rivas and C. Serra, *J. Phys. Chem. C*, 2010, **114**, 15924–15930.
88 N. Vilar-Vidal, J. R. Rey and M. A. López Quintela, *Small*, 2014, **10**, 3632–3636.
89 N. Vilar-Vidal, J. Rivas and M. A. Lopez-Quintela, *Phys. Chem. Chem. Phys.*, 2014, **16**, 26427–26430.
90 S. Huseyinova, J. Blanco, F. G. Requejo, J. M. Ramallo-López, M. C. Blanco, D. Buceta and M. A. López-Quintela, *J. Phys. Chem. C*, 2016, **120**, 15902–15908.
91 X. Yuan, Z. Luo, Q. Zhang, X. Zhang, Y. Zheng, J. Y. Lee and J. Xie, *ACS Nano*, 2011, **5**, 8800–8808.
92 X. Jia, J. Li and E. Wang, *Small*, 2013, **9**, 3873–3879.
93 Z. Li, S. Guo and C. Lu, *Analyst*, 2015, **140**, 2719–2725.
94 C. Vázquez-Vázquez, M. Bañobre-López, A. Mitra, M. A. López-Quintela and J. Rivas, *Langmuir*, 2009, **25**, 8208–8216.
95 H. Kawasaki, Y. Kosaka, Y. Myoujin, T. Narushima, T. Yonezawa and R. Arakawa, *Chem. Commun.*, 2011, **47**, 7740–7742.
96 O. P. Siwach and P. Sen, *J. Nanopart. Res.*, 2008, **10**, 107–114.
97 F. Gao, P. Cai, W. Yang, J. Xue, L. Gao, R. Liu, Y. Wang, Y. Zhao, X. He, L. Zhao, G. Huang, F. Wu, Y. Zhao, Z. Chai and X. Gao, *ACS Nano*, 2015, **9**, 4976–4986.
98 S. Ghosh, N. K. Das, U. Anand and S. Mukherjee, *J. Phys. Chem. Lett.*, 2015, **6**, 1293–1298.
99 C. Wang, S. Shu, Y. Yao and Q. Song, *RSC Adv.*, 2015, **5**, 101599.
100 T. Zhao, X.-W. He, W.-Y. Li and Y.-K. Zhang, *J. Mater. Chem. B*, 2015, **3**, 2388–2394.
101 X. Yang, Y. Feng, S. Zhu, Y. Luo, Y. Zhuo and Y. Dou, *Anal. Chim. Acta*, 2014, **847**, 49–54.
102 X. J. Zhao and C. Z. Huang, *New J. Chem.*, 2014, **38**, 3673–3677.
103 Z. Wu and R. Jin, *Nano Lett.*, 2010, **10**, 2568–2573.
104 Y. Ling, J. J. Wu, Z. F. Gao, N. B. Li and H. Q. Luo, *J. Phys. Chem. C*, 2015, **119**, 27173–27177.
105 S. Kalytchuk, O. Zhovtiuk and A. L. Rogach, *Appl. Phys. Lett.*, 2013, **103**, 103105.
106 J. Luo, Z. Xie, J. W. Y. Lam, L. Cheng, H. Chen, C. Qiu, H. S. Kwok, X. Zhan, Y. Liu, D. Zhu and B. Z. Tang, *Chem. Commun.*, 2001, 1740–1741.
107 P.-C. Chen, Y.-C. Li, J.-Y. Ma, J.-Y. Huang, C.-F. Chen and H.-T. Chang, *Sci. Rep.*, 2016, **6**, 24882.
108 Z. Wu, J. Liu, Y. Gao, H. Liu, T. Li, H. Zou, Z. Wang, K. Zhang, Y. Wang, H. Zhang and B. Yang, *J. Am. Chem. Soc.*, 2015, **137**, 12906–12913.
109 Z. Luo, X. Yuan, Y. Yu, Q. Zhang, D. T. Leong, J. Y. Lee and J. Xie, *J. Am. Chem. Soc.*, 2012, **134**, 16662–16670.
110 P. Shieh, M. J. Hangauer and C. R. Bertozzi, *J. Am. Chem. Soc.*, 2012, **134**, 17428–17431.
111 C. Wu, B. Bull, C. Szymanski, K. Christensen and J. McNeill, *ACS Nano*, 2008, **2**, 2415–2423.
112 C. Wang, Y. Yao and Q. Song, *Colloids Surf., B*, 2016, **140**, 373–381.
113 J. R. Bhamore, S. Jha, A. K. Mungara, R. K. Singhal, D. Sonkeshariya and S. K. Kailasa, *Biosens. Bioelectron.*, 2016, **80**, 243–248.
114 Z. Xia, Z. Xu, M. Chen and Q. Liu, *Dalton Trans.*, 2016, **45**, 11214–11232.
115 H. Terraschke and C. Wickleder, *Chem. Rev.*, 2015, **115**, 11352–11378.
116 H. A. Höppe, *Angew. Chem., Int. Ed.*, 2009, **48**, 3572–3582.
117 J. Liu, Z. Wu, T. Li, D. Zhou, K. Zhang, Y. Sheng, J. Cui, H. Zhang and B. Yang, *Nanoscale*, 2016, **8**, 395–402.
118 Z. Wang, B. Chen, M. Zhu, S. V. Kershaw, C. Zhi, H. Zhong and A. L. Rogach, *ACS Appl. Mater. Interfaces*, 2016, **8**, 33993–33998.
119 X. Gao, S. He, C. Zhang, C. Du, X. Chen, W. Xing, S. Chen, A. Clayborne and W. Chen, *Adv. Sci.*, 2016, **3**, 1600126.

